Talanta 116 (2013) 217–222

Contents lists available at ScienceDirect

Talanta

journal homepage: www.elsevier.com/locate/talanta

Calibration of membrane inlet mass spectrometric measurements of dissolved gases: Differences in the responses of polymer and nano-composite membranes to variations in ionic strength

L.D. Miranda [a,*], R.H. Byrne [a], R.T. Short [b], R.J. Bell [c]

[a] *College of Marine Science, University of South Florida, 140 Seventh Avenue South, St. Petersburg, FL 33701, United States*
[b] *SRI International, 450 Eighth Avenue SE, St. Petersburg, FL 33701, United States*
[c] *Vancouver Island University, 900 Fifth Street, Nanaimo, BC, Canada*

A R T I C L E I N F O

Article history:
Received 26 February 2013
Received in revised form
3 May 2013
Accepted 9 May 2013
Available online 20 May 2013

Keywords:
Membrane introduction mass spectrometry
Nano-composite membranes
Polydimethylsiloxane
MIMS calibrations
Salting-out coefficients
Pervaporation

A B S T R A C T

This work examines the transmission behavior of aqueous dissolved methane, nitrogen, argon and carbon dioxide through two types of membranes: a polysiloxane nano-composite (PNC) membrane and a conventional polydimethylsiloxane (PDMS) membrane. Transmission properties at 30 °C were examined by membrane introduction mass spectrometry (MIMS) at nearly constant gas partial pressures in NaCl solutions over a range of ionic strength (0–1 molal). Gas flow rates were examined as a function of dissolved gas concentrations using the Setschenow equation. Although MIMS measurements with PDMS and PNC membranes produced signal responses that were directly proportional to aqueous dissolved gas concentrations, the proportionalities varied with ionic strength and were distinctly different for the two types of membranes. With the exception of carbon dioxide, the PNC membrane had membrane salting coefficients quite similar to Setschenow coefficients reported for gases in aqueous solution. In contrast, the PDMS membrane had membrane salting coefficients that were generally smaller than the corresponding Setschenow gas coefficient for each gas. Differences between Setschenow coefficients and membrane salting coefficients lead to MIMS calibrations (gas-flow vs. gas-concentration proportionalities) that vary with ionic strength. Accordingly, gas-flow vs. gas-concentration relationships for MIMS measurements with PDMS membranes are significantly dependent on ionic strength. In contrast, for PNC membranes, flow vs. concentration relationships are independent (argon, methane, nitrogen) or weakly dependent (CO_2) on ionic strength. Comparisons of gas Setschenow and membrane salting coefficients can be used to quantitatively describe the dependence of membrane gas-flow on gas-concentrations and ionic strength for both PDMS and PNC membranes.

1. Introduction

Measurement of gas concentrations in aqueous solution is of great importance in a wide variety of scientific, regulatory and commercial applications [1–5]. Detection and quantification of dissolved gases often involves the use of membranes in conjunction with colorimetric pH indicator techniques, polarography or mass spectrometry [1,2,6,7]. Colorimetric and polarographic techniques generally allow measurement of a single gas in solution [6,7], while mass spectrometry facilitates measurements of multiple gaseous components simultaneously [1,2]. As a second important distinction between mass spectrometric measurements of gas concentrations and other membrane-based techniques, membrane introduction mass spectrometry (MIMS) involves measurement of flow rates [8], while other procedures are based on chemical equilibrations. As a result, MIMS can not only provide comprehensive measurements of a variety of gases in solution but can also make measurements on much shorter time scales than are required by equilibrium techniques.

The responses of MIMS systems are strongly regulated by membrane permeability properties. The permeability of polydimethylsiloxane (PDMS), a frequently preferred membrane material, is strongly influenced by gas partitioning between the solution phase and the vapor phase through a process known as pervaporation. This process can be used to describe transmission properties of dissolved gases through the membrane interface into the detector. Ordinarily, MIMS measurements are performed at atmospheric pressure, but the substantial utility of this technique has also led to its in situ employment at hydrostatic pressures greater than one atmosphere [9–13]. At higher hydrostatic pressures, conventional PDMS membranes have been reported to demonstrate variable permeability properties [14,15].

---

* Corresponding author. Tel.: +1 85 044 54875.
E-mail addresses: luisdmiranda@hotmail.com, ldmirand@mail.usf.edu (L.D. Miranda).

0039-9140/$ - see front matter Published by Elsevier B.V.
http://dx.doi.org/10.1016/j.talanta.2013.05.014

Miranda et al. [16] recently described the gas transmission characteristics of polysiloxane nano-composite (PNC) membranes that were coupled to the inlet system of a mass spectrometer. The gas transmission properties of PNC membranes were compared to those of a conventional PDMS membrane over a range of hydrostatic pressures. The PDMS membrane exhibited compression of its siloxane matrix when hydrostatic pressure was increased, and exhibited hysteresis when hydrostatic pressure was subsequently decreased. Thus the permeability properties of the PDMS membrane are influenced by hydrostatic pressure in a manner that presents substantial challenges to quantitative calibration. In contrast, the transmission properties of the PNC membranes constructed by Miranda et al. [16] demonstrated little if any response to changes in hydrostatic pressure.

Having previously shown that PNC membranes are much less susceptible to hydrostatic pressure-induced variation in permeation properties than PDMS membranes, this work examines the comparative gas-transmission properties of PNC membranes and PDMS membranes over an environmentally-relevant range of ionic strengths. Using gas mixtures with constant compositions, gas concentrations in equilibrated solutions were varied (i.e. decreased) with increasing NaCl concentration (ionic strength) while gas partial pressures were essentially constant. This investigation shows that variations in ionic strength exert much smaller influences on the permeation of gases through PNC membranes than conventional PDMS membranes. Additionally, it is shown that the influence on ionic strength on MIMS calibrations (gas-flow vs. gas-concentration) can be well-described in terms of differences between membrane salting coefficients and Setschenow coefficients for both PDMS and PNC membranes.

2. Theory

2.1. Gas solubility theory

The concentration of gas ($C_{(aq)}$) in an aqueous solution when a gas phase and solution phase are in equilibrium can be described using Henry's Law [17]

$$C_{(aq)} = \beta P_p \tag{1}$$

where β is the solubility constant for a gas in an aqueous solution and P_p is the partial pressure of a gas in equilibrium with the solution. Gas concentrations in solution can be expressed in terms of gas activity coefficients (γ_G) via the following relationship: $C_{(aq)} = a_G/\gamma_G$, where a_G is the activity of a gas in solution. The concentrations (or solubility) of gases in aqueous solution are decreased by addition of salts (i.e. the salting-out effect) as γ_G increases with salt content. The relevant measure of comparative concentrations of a particular gas in solutions of variable salt content is the ionic strength, I [18]. At constant temperature and partial pressure, the comparative solubility of a gas over a range of ionic strength can be well described using the Setschenow equation [19,20]:

$$\ln(\beta^\circ/\beta_s) = \ln(\gamma_{G,s}) = k_s I \tag{2}$$

where β° and β_s are solubility coefficients for a gas in pure water ($I=0$) and a solution with ionic strength (I), $\gamma_{G,s}$ is the activity coefficient of a gas in a solution with ionic strength and k_s is the salting-out coefficient for a given gas.

2.2. Membrane introduction mass spectrometry (MIMS) theory

Membranes (e.g. PDMS and PNC) act as interfaces between sample solutions and the vacuum of a mass spectrometer. Transport through the membrane (as a pervaporation process) is induced by maintaining the vapor pressure on the permeate side at a lower vapor pressure than in the feed liquid. The pervaporation process involves a sequence of three steps: (i) selective sorption of analyte(s) into the membrane on the feed side, (ii) diffusion of the analyte(s) through the membrane, and (iii) desorption of the analyte(s) into a vapor phase on the permeate side of the membrane [21]. The solution–diffusion model assumes that, at the solution/membrane interface the activity of an analyte in the feed liquid is equal to the activity of the analyte in the membrane [22]. The activity (a_m) of an analyte in the membrane on the feed (solution) side of the membrane is given as: $a_m = \gamma_m C_m$, where γ_m and C_m are the activity coefficient and the concentration of an analyte in the membrane at the solution/membrane interface. Under steady-state conditions, the ion current (Φ) measured by the mass spectrometer is directly proportional to the flow (F) of an analyte across a membrane and can be described by the following equations [23–33]:

$$F = \Phi\omega \tag{3a}$$

$$F = AD(a_m/L) \tag{3b}$$

where ω is a proportionality constant, A is the membrane surface area, D is the analyte diffusion coefficient, and L is the membrane thickness.

3. Experimental procedures

The PDMS membrane used in this work was of conventional design, with surface area and membrane thickness comparable to those of PDMS membranes reported by other research groups [23,24,34,35]. In contrast, the PNC membranes used in this work were fabricated using novel techniques.

Synthesis and characterization of polysiloxane nano-composite (PNC) membranes are described in Miranda et al. [16]. An overview of the process is given as follows: an anodic aluminum oxide (AAO) membrane was mounted on a stainless steel frit and secured on a membrane module with vacuum epoxy. A thin polysiloxane film was mechanically coated on the surface of the AAO using a room-temperature-vulcanizing silicon rubber. Two membranes were created in this manner and mounted in series on a custom-made manifold membrane module. The AAO membranes were 60 μm thick and had pores with an average diameter of 200 nm. Polysiloxane films were uniformly deposited across the upper surface of the AAO membranes and, on average, were 11 μm thick. The cumulative area of the PNC membranes was ~6.2 mm^2.

The PDMS membrane (Specialty Manufacturing Inc.) used in this work was 127 μm thick and had a total area of 2.8 cm^2. The PDMS membrane was mounted on a custom-made membrane module (Fig. 1).

Mass spectrometry measurements were conducted using an experimental configuration similar to that described in Miranda et al. [16]. The PNC and PDMS membrane modules were connected individually to a quadrupole mass spectrometer (Inficon, Transpector 2.0 Gas Analyzer System) via a Swagelok fitting. Solutions were pumped through the membrane modules using a peristaltic pump. The peristaltic pump was placed downstream of the membrane module. MIMS measurements were made using a Faraday cup detector.

Four solutions, each in a (500 ml) volumetric flask, were placed in a constant temperature water bath (30 °C). One set of solutions, deionized (DI) water and a sodium chloride solution, were simultaneously equilibrated at atmospheric pressure with a gas mixture (Airgas certified) while the other set (of similar solution composition) were simultaneously equilibrated at atmospheric pressure with a baseline gas. Measurements were obtained using gas mixtures containing methane (CH_4), argon (Ar), carbon dioxide

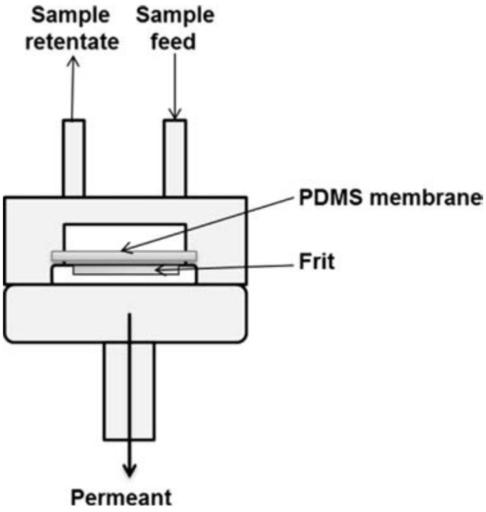

Fig. 1. The above image shows the diagram of the PDMS membrane module. For comparison, the diagram of the PNC membrane module can be seen in Miranda et al. [16].

(CO_2), and nitrogen (N_2). Gas mixtures had variable CH_4, Ar and CO_2 concentrations in the parts-per-million, parts-per-thousand and parts-per-hundred levels with N_2 as the balance gas. Baseline values for CH_4, Ar and CO_2 measurements where obtained using an ultrapure N_2 gas (Airgas certified) bubbled through each experimental solution. The baseline gas had CH_4, Ar and CO_2 at lower parts-per-billion levels, well below the detection limits of our mass spectrometer. In the case of N_2, baselines were measured prior to each experimental run by degassing the solution at sample flow rate equal to zero [16]. Sufficient time was allowed for the sample to be thoroughly degased at the membrane interface. This baseline procedure for N_2 gas was performed solely using degassed solutions rather than solutions that had been equilibrated with gases. Gas streams were hydrated by bubbling through a flask that contained DI water before entering the volumetric flasks that contained the DI and NaCl solutions. DI and NaCl solutions were acidified to a pH≈2 with concentrated HCl in order to prevent the formation of HCO_3^- and CO_3^{2-} that would otherwise occur in the presence of dissolved CO_2.

The ion currents (Φ) produced by diffusion of CH_4, N_2, Ar, and CO_2 through the PDMS and PNC membranes were analyzed at m/z ratios of 15, 28, 40, and 44, respectively. Experimental runs were performed at steady rates of flow (F). Gas flow measurements were obtained when mass spectrometer signals (Φ') attained steady-state. Measurements were averaged for 100 scans and then baseline-subtracted to produce an ion current: $\Phi = \Phi' - \Phi'_{(\text{baseline})}$, where Φ' is the ion current obtained using a solution equilibrated with the gas mixture at a specific ionic strength and $\Phi'_{(\text{baseline})}$ is the ion current of the same gas observed using a solution equilibrated with the baseline gas at the same ionic strength (i.e. for CH_4, Ar, and CO_2) or the degassed solution (i.e. for N_2). For each measured Φ_s value obtained at ionic strength I, (0.1, 0.5 and 1.0 molal) a baseline-corrected ion current (Φ°) at $I=0$ was also obtained using DI water. This procedure was repeated using NaCl solutions and DI equilibrated with various gas mixtures.

4. Results and discussion

In order to directly examine the dependence of gas flow on ionic strength, the flow (F°) of each gas dissolved in pure water ($I=0$) was ratioed to the flow of a gas (F_s) observed at each ionic strength (I). Plots of $\ln(F^\circ/F_s)$ vs. I (where $F^\circ/F_s = \Phi^\circ/\Phi_s$) for the PDMS and PNC membranes are shown in Fig. 2.

The plots of $\ln(F^\circ/F_s)$ vs. I, shown in Fig. 2, are highly linear and are consistent with expected gas solubility behavior based on the Setschenow equation (i.e. Eq. (2)). Fig. 2 demonstrates that the influence of ionic strength on gas flow for both types of membranes is well described by the following equation:

$$\ln(F^\circ/F_s) = k_m I \tag{4}$$

where k_m can be termed a membrane salting coefficient [36]. Fig. 2 shows that the membrane salting coefficients of the PDMS membrane are different than those of the PNC membranes. The PDMS and PNC membrane salting coefficients (k_m) obtained using Eq. (4) are directly compared in Table 1. Setschenow salting-out coefficients (k_s) for sea water are also presented in Table 1. The selected gas salting-out coefficients in Table 1 were chosen based on the high degree of precision in the selected works [37–40]. For the PNC membranes, Table 1 shows that, for CH_4, N_2 and Ar, k_m and k_s are essentially identical. In contrast, the k_m value obtained for CO_2 with the PNC membranes is somewhat smaller than the k_s value for sea water. For the PDMS membrane, k_m values are consistently smaller than gas salting-out coefficients (k_s).

Gas flow can be related to gas concentrations and ionic strength by combining Eqs. (1), (2) and (4). At constant temperature and partial pressure, Eqs. (1) and (2) can be combined and written as follows:

$$\ln(C^\circ_{(aq)}/C_{(aq),s}) = k_s I \tag{5}$$

where $C^\circ_{(aq)}$ and $C_{(aq),s}$ are the concentrations of a gas dissolved in pure water and a solution with ionic strength. Eqs. (4) and (5) can then be combined and written as

$$\ln(F^\circ/F_s) - \ln(C^\circ_{(aq)}/C_{(aq),s}) = (k_m - k_s)I \tag{6}$$

Rearrangement of Eq. (6) produces the following two equations:

$$F_s = C_{(aq),s}(F^\circ/C^\circ_{(aq)})e^{(k_s - k_m)I} \tag{7a}$$

$$C_{(aq),s} = F_s(C^\circ_{(aq)}/F^\circ)e^{(k_m - k_s)I} \tag{7b}$$

The exponential terms in Eq. (7), $e^{(k_s - k_m)I}$ and $e^{(k_m - k_s)I}$, demonstrate that relationships between gas-flow and gas-concentration are explicitly influenced by ionic strength unless Setschenow coefficients and membrane salting coefficients are identical. Examination of Table 1 shows that $k_s \geq k_m$. As a result Eq. (7a) shows that, for measurements made using PDMS membranes, $F_s/C_{(aq),s}$ ratios (i.e. slopes of ion currents vs. gas-concentration) will consistently increase with ionic strength. In contrast, for measurements made using PNC membranes, $F_s/C_{(aq),s}$ ratios are independent of ionic strength for methane, nitrogen and argon, but not carbon dioxide. Table 2 shows flow vs. concentration results at zero ionic strength normalized to the surface area of each membrane. For the PNC membrane, the zero ionic strength results shown in the table will not vary with ionic strength except in the case of CO_2. The results in Table 2 also show that F_s vs. $C_{(aq),s}$ for the PDMS membrane are uniformly higher than the corresponding slopes for the PNC membrane. Since F_s vs. $C_{(aq),s}$ slopes for the PDMS membranes increase with ionic strength, the transmission properties of the two membranes will increasingly diverge with increasing ionic strength.

Table 3 shows values of $e^{(k_s - k_m)I}$ for both membranes at each of the ionic strengths in this investigation. The results for CO_2 in the table show that F_s vs. $C_{(aq),s}$ calibration slopes for PDMS membranes will be 7.6% higher at ionic strength 1 than at ionic strength zero. A smaller effect (~2.9%) for CO_2 is observed for the PNC membrane. The results shown in Table 3 indicate that gas-flow vs. gas-concentration relationships should be interpreted using Eq. (7) when measurements are made over a range of ionic strengths. This observation will become particularly important when MIMS systems are used in estuaries over a range of salinities.

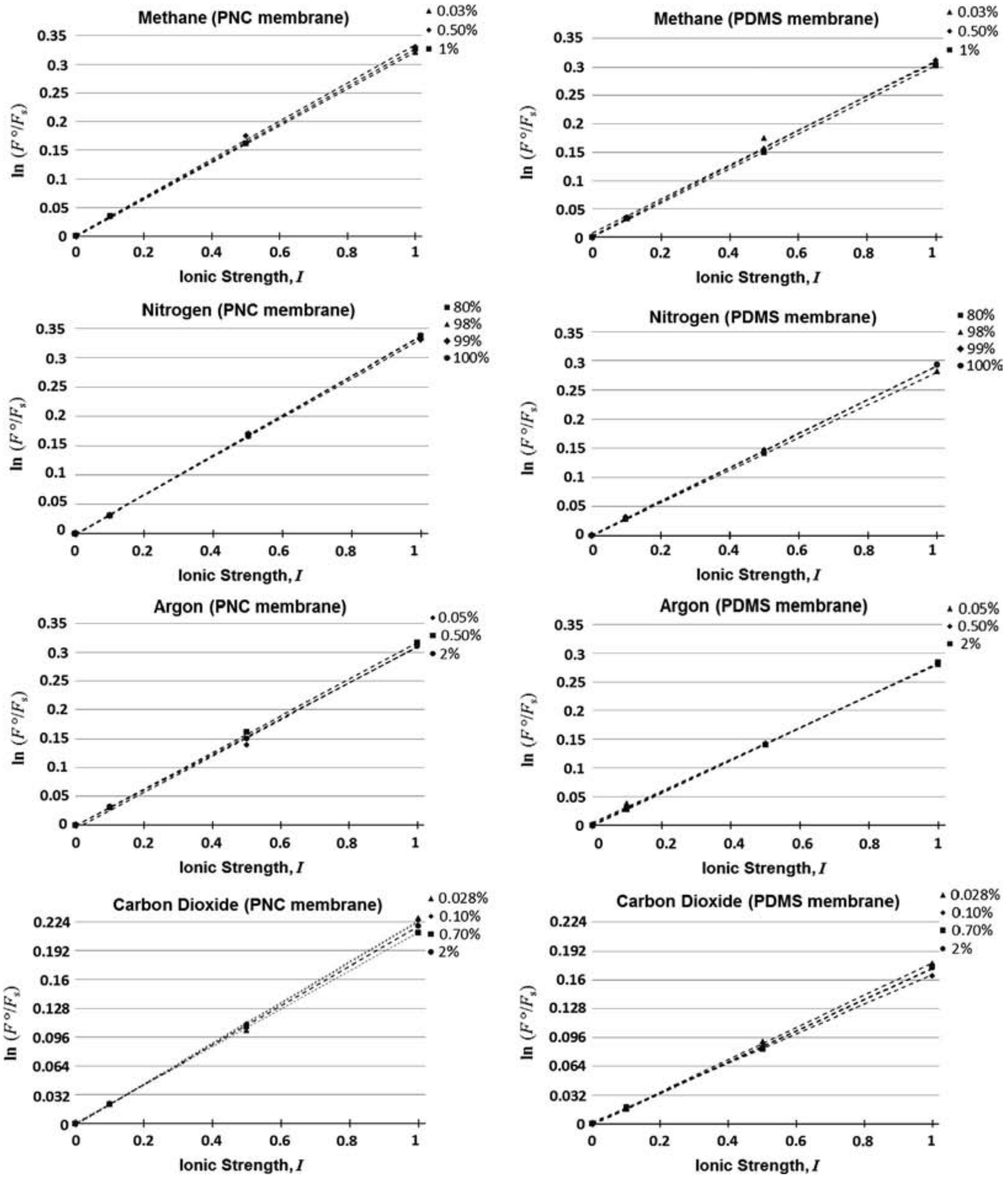

Fig. 2. Gas flow rates through PDMS and PNC membranes are plotted as ln(F°/F_s) vs. I. Percent mole fractions (i.e. mole fraction × 100) for each gas in the gas mixtures are shown at the upper right of each figure. A best fit line for the data obtained at each percent gas concentration for the different ionic strengths is shown as (—).

Table 1
Membrane salting coefficients for gases permeating through PDMS and PNC membranes at 30 °C and salting-out coefficients for gases in sea water.

Gas	PNC membranes, k_m	PDMS membrane, k_m	Salting-out coefficients, k_s
CH_4	0.331 ± 0.011	0.319 ± 0.019	0.331 ± 0.001[a]
N_2	0.335 ± 0.005	0.289 ± 0.007	0.334 ± 0.001[b]
Ar	0.313 ± 0.009	0.284 ± 0.008	0.310 ± 0.001[b]
CO_2	0.218 ± 0.006	0.173 ± 0.008	0.247 ± 0.001[c]

Values of k_m were calculated using Eq. (4). Salting-out coefficients (k_s, kg-H_2O mol^{-1}) were calculated using Eq. (2) and solubility coefficients reported previously at 30 °C within a 0–15 range of salinity from the following data sources.

[a] The CH_4 coefficient was derived using solubility coefficients presented by Wiesenburg and Guinasso [37].

[b] N_2 and Ar coefficients were derived from solubility coefficients presented by Weiss [39].

[c] The CO_2 coefficient was derived using the solubility coefficients presented by Weiss [40]. Na^+ and Cl^- ions are the two major ion components of sea water and, although salting-out coefficients are somewhat influenced by medium composition, the salting-out coefficients of sea water shown above can be used as reasonable representation of salting-out coefficients for NaCl solutions. Additional constants used to correct solubility coefficients to mole per kg-H_2O units were found in the CRC press (Physical Constants of Inorganic Compounds Section). The ionic strength of sea water can be simulated with NaCl solutions and related to salinity using the following equation [41]: $I = m_{NaCl} = 19.924\ S‰/(1000–1.005\ S‰)$, where m_{NaCl} is the molality of the NaCl solution and S‰ is the salinity in parts per thousand.

Table 2
Observed $F^\circ/C^\circ_{(aq)}$ slopes for CH_4, N_2, Ar and CO_2 normalized to the membrane surface area of the PDMS and PNC membranes where $(F^\circ/C^\circ_{(aq)})/A$. The total surface area of the PNC membranes is 6.2 mm^2 and 280 mm^2 for the PDMS membrane. (units: $C_{(aq)}$=μmol kg-H_2O^{-1}, A=mm^2, gas-flow rates were observed as a function of ion current, where Φ=A).

Gas	PNC membrane ($\times 10^{-15}$)	PDMS membrane ($\times 10^{-15}$)
CH_4	1.542	1.732
N_2	1.777	1.837
Ar	1.225	2.024
CO_2	0.302	0.438

Table 3
The exponential term in Eq. (7a) (i.e. $e^{(k_s - k_m)\,I}$) is shown explicitly at several ionic strengths.

	PNC membrane				PDMS membrane			
I	CH_4	N_2	Ar	CO_2	CH_4	N_2	Ar	CO_2
0.1 m NaCl	1.000	0.999	0.999	1.002	1.001	1.004	1.002	1.007
0.5 m NaCl	1.000	0.999	0.998	1.014	1.006	1.022	1.013	1.037
1.0 m NaCl	1.000	0.999	0.997	1.029	1.012	1.046	1.026	1.076

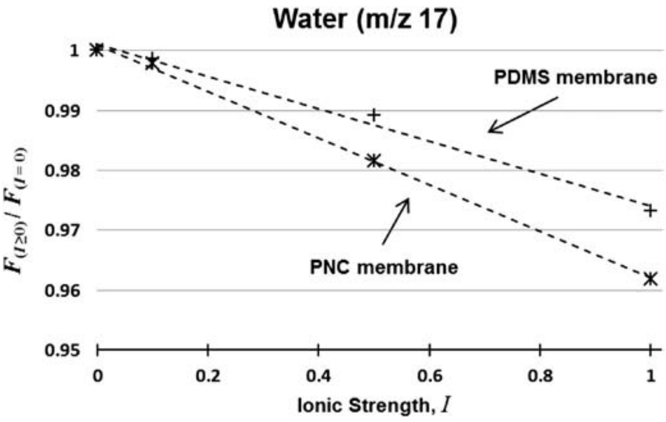

Fig. 3. Water flow through the PDMS and PNC membranes over a 0 to 1 molal range of ionic strength. The flow of water was plotted as F/F° vs. I. The transmission of water through the PDMS and PNC membranes was measured by the mass spectrometer at m/z 17.

In addition to our investigation of comparative gas permeation for the two types of membranes, our work demonstrated that PDMS and PNC membranes exhibited different water permeation characteristics. Fig. 3 shows, for each membrane, water flow plotted as F/F° vs. ionic strength where F° represents water flow at zero ionic strength. The influence of ionic strength on water flow is different for the two types of membranes. Furthermore, it was observed that the overall water flow for the two membranes, normalized to membrane surface area, is quite different. For the PNC membrane the area-normalized water flow at I=0 was 1.285×10^{-11} A mm^{-2} whereas, for the PDMS membrane the area-normalized water flow at I=0 was 0.803×10^{-11} A mm^{-2} (water-flow rates were expressed in terms of ion current, where Φ=A).

5. Conclusions

The close correspondence between gas-flow rates and gas-concentrations that was obtained with the PNC membrane over a range of ionic strength indicates that calibration and use of MIMS with PNC membranes is inherently simpler than is the case for measurements using PDMS membranes. This makes PNC membranes inherently desirable for applications of MIMS in environments with large salinity gradients and variable hydrostatic pressures.

Our investigation develops a simple quantitative procedure for calibrating MIMS devices for use in salinity or ionic strength gradients. Our observations demonstrate that, toward the objective of MIMS measurements of gas concentrations in estuaries, MIMS calibrations should be performed at a minimum of two ionic strengths. In the simplest case, observations of ion current and gas concentration ratios at ionic strengths equal to 0 and 1 molal will allow direct calculation of the k_s–k_m term in Eq. (6). This difference between k_s and k_m provides (via Eq. (7)) a quantitative account of the influence of ionic strength on the responses of MIMS systems in salinity gradients.

Our results are consistent with the conclusion that MIMS gas-flow vs. gas-concentration relationships are dependent on ionic strength because the activity of water in membranes is dependent on the ionic strength of the solution being sampled. Variations of water activity in PDMS membranes significantly influence pervaporation characteristics of gases through the membrane. For the PNC membrane this influence was significant only for CO_2.

As the activity of water decreases with increasing ionic strength (Fig. 3) it is seen that rates of water-flow through the PDMS and PNC membranes substantially decrease. As such, the simple relationships obtained between water flow and ionic strength (Fig. 3) for the two types of membranes suggest that measurements of water flow rates can be used as a means of estimating the ionic strengths that are required in the Eqs. (6) and (7) concentration vs. flow calibrations.

During our work it was observed that baseline values for CH_4, Ar and CO_2 were higher in DI water and progressively lower with increasing ionic strength (results not shown). This observation indicates that baseline values for MIMS calibrations are dependent on salinity and ionic strength. For MIMS measurements in salinity gradients calibration procedures should therefore include appropriate measurements of baseline values (i.e. using ultrapure N_2 gas) over a range of ionic strength. For gases at very low concentrations, lower quality baseline gases produce unreliable baseline values and less consistent membrane salting coefficients (results not shown).

A Supplementary information (SI) section associated with this paper provides an interpretation of Eq. (6) in terms of the physical-chemical characteristics of membranes. The SI section examines how the results presented in Table 3 are directly related to membrane sorption properties.

Acknowledgments

- Support by the NSF Florida-Georgia Louis Stokes Alliance for Minority Participation (FGLSAMP) Bridge to the Doctorate supplements awards HRD #0217675 and GEO #0503536 is gratefully acknowledged.
- This project benefitted from support by the Alfred P. Sloan Minority Ph.D. Fellowship program.
- This work was supported by the Office of Naval Research through Grants N00014-03-1-0479, N00014-03-1-0612 and N00014-10-1-0787 and SRI Contract N00014-07-C-0720.

Appendix A. Supporting information

Supplementary data associated with this article can be found in the online version at http://dx.doi.org/10.1016/j.talanta.2013.05.014. The authors would like to take an opportunity to address some discrepancies published in Miranda et al., J. Membr. Sci. 385 (2011)

49-56. The term flux was misused throughout the text and it should instead be substituted for the term flow.

References

[1] R.C. Hamme, S.R. Emerson, Deep-Sea Res. 51 (2004) 1517–1528.
[2] T.M. Kana, C. Darkangelo, M.D. Hunt, J.B. Oldham, G.E. Bennett, J.C. Cornwell, Anal. Chem. 66 (1994) 4166–4170.
[3] K.J. Flynn, J.C. Blackford, M.E. Baird, J.A. Raven, D.R. Clark, J. Beardall, C. Brownlee, H. Fabian, G.L. Wheeler, Nat. Climate Change 2 (2012) 510–513.
[4] S.G. Osborn, A. Vengosh, N.R. Warner, R.B. Jackson, PMAS 108 (2011) 8172–8176.
[5] S. Bohátka, I. Futó, I. Gál, J. Gál, G. Langer, J. Molnár, A. Paál, G. Pintér, M. Simon, J. Szádai, G. Székely, Vacuum 44 (1993) 669–671.
[6] M.D. DeGrandpre, T.R. Hammar, S.P. Smith, F.L. Sayles, Limnol. Oceanogr. 40 (1995) 969–975.
[7] H.Y. Wang, X-M. Li, Biosensors 4 (1989) 273–285.
[8] G. Hoch, B. Kok, Arch. Biochem. Biophys. 101 (1963) 160–170.
[9] R. Camilli, A.N. Duryea, Environ. Sci. Technol. 43 (2009) 5014–5021.
[10] R. Camilli, B. Bingham, C.M. Reddy, R.K. Nelson, A.N. Duryea, Mar. Pollut. Bull. 58 (2009) 1505–1513.
[11] R. Camilli, C.M. Reddy, D.R. Yoerger, B.A.S. van Mooy, M.V. Jakuba, J.C. Kinsey, C.P. McIntyre, S.P. Sylva, J.V. Maloney, Science 330 (2010) 201–204.
[12] R.T. Short, D.P. Fries, S.K. Toler, C.E. Lembke, R.H. Byrne, Meas. Sci. Technol. 10 (1999) 1195–1201.
[13] R.T. Short, D.P. Fries, M.L. Kerr, C.E. Lembke, S.K. Toler, P.G. Wenner, R.H. Byrne, J. Am. Soc. Mass Spectrom. 12 (2001) 676–682.
[14] I. Futó, H. Degn, Anal. Chim. Acta 294 (1994) 177–184.
[15] R.J. Bell, R.T. Short, F.H.W. van Amerom, R.H. Byrne, Environ. Sci. Technol. 41 (2007) 8123–8128.
[16] L.D. Miranda, R.J. Bell, R.T. Short, F.H.W. van Amerom, R.H. Byrne, J. Membr. Sci. 385 (2011) 49–56.
[17] M.E.Q. Pilson, An Introduction to the Chemistry of the Sea, Prentice Hall, New Jersey, 1998.
[18] W. Stumm, J.J. Morgan, Aquatic Chemistry—Chemical Equilibria and Rates in Natural Waters, 3rd ed., John Wiley & Sons, New York101.
[19] F. Millero, Mar. Chem. 70 (2000) 5–22.
[20] F.J. Millero, D.R. Schreiber, Am. J. Sci. 282 (1982) 1508–1540.
[21] M. Mulder, Basic Principles of Membrane Technology, 2nd ed., Kluwer Academic Publishers, Netherlands210–279.
[22] J.G. Wijmans, R.W. Baker, J. Membr. Sci. 107 (1995) 1–21.
[23] N. Srinivasan, R.C. Johnson, N. Kasthurikrishnan, P. Wong, R.G. Cooks, Anal. Chim. Acta 350 (1997) 257–271.
[24] R.C. Johnson, R.G. Cooks, T.M. Allen, M.E. Cisper, P.H. Hemberger, Mass Spectrom. Rev. 19 (2000) 1–37.
[25] M.A. LaPack, J.C. Tou, C.G. Enke, Anal. Chem. 62 (1990) 1265–1271.
[26] W. Kujawski, S.R. Krajewski, Sep. Purif. Technol. 57 (2007) 495–501.
[27] K.W. Boddeker, G. Bengtson, J. Membr. Sci 53 (1990) 143–158.
[28] F. Lipnizki, S. Hausmanns, R.W. Field, J. Membr. Sci 228 (2004) 129–138.
[29] U. Cocchini, C. Nicolella, A.G. Livingston, J. Membr. Sci 162 (1999) 57–72.
[30] V. Freger, E. Korin, J. Wisniak, E. Korngold, J. Membr. Sci 128 (1997) 151–162.
[31] J. Marszalek, W.L. Kaminski, Chem. Process. Eng. 33 (2012) 131–140.
[32] V. Garcia, E. Pongracz, E. Muurinen, R.L. Keiski, Desalination 241 (2009) 201–211.
[33] V. Garcia, E. Pongracz, E. Muurinen, R.L. Keiski, J. Membr. Sci 326 (2009) 92–102.
[34] H. Ørsnes, S. Bohatka, H. Degn, Rapid Commun. Mass Spectrom. 11 (1997) 1736–1738.
[35] P.D. Tortell, Limnol. Oceanogr.: Methods 3 (2005) 24–37.
[36] R.J. Bell, R.T. Short, R.H. Byrne, Limnol. Oceanogr.: Methods 9 (2011) 164–175.
[37] D.A. Wiesenburg, N.L. Guinasso, J. Chem. Eng. Data 24 (1979) 356–360.
[38] S. Yamamoto, J.B. Alcauskas, T.E. Crozier, J. Chem. Eng. Data 21 (1976) 78–80.
[39] R.F. Weiss, Deep-Sea Res. 17 (1970) 721–735.
[40] R.F. Weiss, Mar. Chem. 2 (1974) 203–215.
[41] A.G. Dickson, C. Goyet, Handbook of Methods for the Analysis of the Various Parameters of the Carbon Dioxide System in Sea Water, (1994) Version 2. ORNL/CDIAC-74 ⟨doi:10.2172/10107773⟩.